

Topical delivery and photodynamic evaluation of a multivesicular liposomal Rose Bengal

Maha Fadel M. Ali

Received: 4 June 2010 / Accepted: 28 October 2010 / Published online: 1 December 2010
© Springer-Verlag London Ltd 2010

Abstract We investigated the pharmaceutical and physico-chemical properties of different multivesicular liposome (MVL) formulations for the delivery of Rose Bengal (RB) into skin layers for topical photodynamic therapy. The drug content, uniformity, spreadability and release kinetics of the optimum hydrogel formulation were studied. Skin penetration of the prepared gels was studied in albino mice using fluorescence microscopy and the photodynamic properties were evaluated. The loading efficiency of MVL ranged from 56% to 79%. In vitro RB release from MVL followed Higuchi's diffusion mechanism and the amount of RB released after 2 h from the optimum MVL (comprising D,L-dipalmitoylphosphatidyl choline, cholesterol and tripalmitin at a molar ratio of 1:0.7:0.1, respectively) was 2.5-fold higher than from the other MVL formulations. The type and concentration of phospholipids did not significantly ($p > 0.05$) affect vesicle size but significantly ($p < 0.05$) increased the encapsulation capacity and thermal properties. RB in hydrogel was spreadable and uniformly distributed. Fluorescence microscopy 30 min after topical application to the skin of mice showed that RB loaded into MVL was significantly ($p < 0.05$) more distributed into the dermal layers than free RB which accumulated in the epidermis. This finding was confirmed by the presence of superficial necrotic cells in histological sections of skin treated with free RB and the presence of RB in the deep dermal layers of sections of skin treated with the MVL-RB formulation and irradiated for 10 min with light of wavelength 550 nm from a light emitting diode at 80 mW. MVL hydrogel is a

promising topical delivery system which allows successful delivery of RB into skin layers for different photodynamic therapies in dermatology.

Keywords Multivesicular liposomes · Rose Bengal · PDT · LED · Hydrogel · Topical delivery

Introduction

Photodynamic therapy (PDT) is an emerging modality for the treatment of neoplastic and non-neoplastic diseases. The photochemical mechanism underlying PDT processes involves absorption of visible radiation by the dye molecules and subsequent formation of reactive intermediates, such as singlet oxygen (1O_2), superoxide anion (O_2^-) and other reactive oxygen species and radicals of the dyes [1, 2]. Rose Bengal (RB) is a potent xanthene photosensitizer that has largely been overlooked as a potential candidate for PDT [3, 4]. The feasibility of topical delivery of RB to the epidermis using hydrophilic formulations has been evaluated, and such formulations have been shown to be able to deliver RB to the epidermis rapidly, selectively and uniformly, with no significant acute cutaneous toxicity in normal skin [5].

However, the low lipid solubility of RB limits its capacity to cross biological barriers such as cell membranes, thus limiting its clinical application. Previous studies on the delivery of photosensitizers for PDT have investigated the use of conventional or modified liposomes. They are excellent carriers for both hydrophobic and hydrophilic photosensitizers for the treatment of tumours by PDT [6–10]. Moreover, they are able to increase concentration of the compound in the epidermis and in the deeper layers of the skin probably through the similarity

M. F. M. Ali (✉)
Pharmaceutical Technology Unit, Department of Medical
Applications of Lasers, National Institute of Laser Enhanced
Sciences, Cairo University,
Cairo, Egypt
e-mail: mahafmali@hotmail.com

of their lipid bilayer to that of the skin [11]. However, conventional liposomes have certain limitations including low entrapment efficiency of water-soluble drugs, stability problems, and release of drugs after a single breach in the external membrane [12]. The low aqueous entrapment precludes effective use of these carriers for hydrophilic drugs [13]. This challenge has been successfully met by the use of multivesicular liposome (MVL) drug-delivery systems [14–16]. MVL systems are characterized structurally by multiple nonconcentric aqueous chambers surrounded by a network of lipid membranes [12]. The general chemical composition of MVL systems comprises a neutral lipid (for example, triolein, tricaprlyene, tripalmitin, trilaureine, tributyrine) as an integral component, which is responsible for the unique multivesicular structure [17, 18]. MVL technology has successfully been used to deliver several small molecules, analgesics, antitumour drugs, and antiviral drugs achieving prolonged therapeutic concentrations [19–22]. Since the structural characteristics of MVL make them ideal vehicles for drug delivery, the aim of this work was to design and characterize MVL loaded with hydrophilic RB (MVL-RB) as an economic and efficient photosensitizer for PDT, and to study skin penetration and the photodynamic efficiency of MVL-RB in the skin of albino mice when delivered in hydrogel formulations for topical use.

Materials and methods

D,L-Dipalmitoylphosphatidyl choline (DPPC), phosphatidyl choline (PC) from soy bean, cholesterol (CHOL), Analar grade chloroform and 4-(2-hydroxyethyl)piperazine-1-ethanesulphonic acid (HEPES) buffer were purchased from Sigma Chemical Co. (St. Louis, MO) and, together with lipids, were used without further purification. TP, RB and free-base lysine (analytical grade) were purchased from Sigma-Aldrich, Buchs, Switzerland. Gel formulations were prepared from 5% carboxymethylcellulose (CMC; Al Nasr Company, Egypt), and 0.2% propyl paraben and 0.1%

methyl paraben of pharmaceutical grade, USP 25 (Normest Co. for Scientific Development, Ramadan City, Egypt).

Preparation of multivesicular liposomes

The MVL-RB formulations were prepared by the reverse phase evaporation technique using a double emulsion (w/o/w) method, described in previous reports [18, 23, 24]. Briefly, an aqueous solution of RB (1 mg/ml) was emulsified with an equal volume of chloroform solution containing an amphipathic lipid (PC/DPPC/CHOL/TP in different molar ratios as shown in Table 1) using a homogenizer (Janke & Kunkel, IKA-Labortechnik, Staufen, Germany) at ambient temperature (23–28°C) for 9 min at 9,000 rpm to produce a w/o primary emulsion, which was then emulsified with a second aqueous solution containing 1.5% glycine/40 mM lysine at 6,000 rpm for 1 min to produce the w/o/w double emulsion. The chloroform was removed under vacuum using a rotary evaporator with flushing nitrogen gas at the surface of the w/o/w emulsion at 37°C, at a gentle speed (50 rpm). The resulting MVL were washed to remove un-entrapped drug and harvested by centrifugation for 15 min at 10,000 g and then resuspended in HEPES-buffered saline at pH 7.4.

In vitro characterization

MVL-RB formulations were characterized for the attributes discussed in the following sections.

Vesicle distribution

Size distribution was determined using an optical microscope (CKX41; Olympus, UK) attached to a colour CCTV camera (WV-CP 240/G; Panasonic System Solutions Suzhou Co., Suzhou, China). MVL formulations (10 µl) were diluted ten times with HEPES-buffered saline and the number of vesicles per cubic millimetre was determined and the vesicles examined for shape and size using a Micrometrics SE/CMOS version 2.6 digital camera system

Table 1 Composition and characterization of MVL formulations. The values are the means \pm SD from three parallel preparations

| MVL-RB formulation | Composition (molar ratios) | | | | Encapsulation efficiency (%) | Size (µm) | RB released after 2 h (µg/ml) |
|--------------------|----------------------------|------|-----|------|------------------------------|----------------|-------------------------------|
| | PC | DPPC | TP | CHOL | | | |
| I | 1 | 0 | 0.2 | 1.5 | 56.67 \pm 0.33 | 2.6 \pm 0.43 | 34.27 \pm 0.1 |
| II | 1 | 0 | 0.1 | 0.7 | 54.61 \pm 2.23 | 4.2 \pm 0.6 | 31.92 \pm 0.09 |
| III | 0 | 1 | 0.2 | 1.5 | 62.7 \pm 3.102* | 3.4 \pm 0.7 | 31.18 \pm 0.15 |
| IV | 0 | 1 | 0.1 | 0.7 | 79 \pm 3.47* | 2.1 \pm 0.5 | 75.9 \pm 0.3 |

* $p < 0.05$, ANOVA/Tukey Kramer test.

(ACCU-SCOPE) and a haemocytometer (Feinoptik, Blankenburg, Germany).

Encapsulation capacity

A 1-ml aliquot of the prepared MVL dispersion was centrifuged at 10,000 *g* for 15 min, the pellets were mixed with 1 ml 1% Triton X-100 in HEPES buffer (pH 7.4) and the clear solution was measured for encapsulated RB applying a previously prepared calibration curve of RB in HEPES buffer (pH 7.4) at a scanning range from 400 to 600 nm. The maximum absorption wavelength of RB was at 544 nm and the curve was done in triplicate. The correlation coefficient (r^2) of the line was 0.999 ± 0.001 and linearity was achieved in range 0.5–50 $\mu\text{g/ml}$. Baseline correction was done using a placebo-dissolved empty MVL dispersion suitably diluted with Triton X-100 to nullify any possible absorption arising from the soluble lipid [25]. For the initial RB concentration, 1 ml of the prepared MVL dispersion was digested with 1 ml 1% Triton X-100 and the RB concentration determined as previously described. The encapsulation capacity was estimated through the following relationship:

$$\text{EC} = \frac{\text{Concentration of loaded RB}}{\text{Initial RB concentration}} \times 100 \quad (1)$$

In vitro drug release profile

The release profile of MVL-encapsulated RB was studied by directly mixing one volume of the MVL suspension (0.5 ml) with nine volumes of HEPES buffer (4.5 ml). The samples were incubated at 37°C with gentle agitation and 1-ml aliquots were withdrawn at 15, 30, 60, 90 and 120 min. For quantification of RB, the aliquots were centrifuged at 10,000 *g* for 15 min and the released RB in the supernatant quantified by UV spectrophotometry as described above. The pellets were resuspended in fresh HEPES buffer and returned back to the samples. The release data were corrected by the dilution factor.

Thermal analysis of MVL using differential scanning calorimetry

Differential scanning calorimetry (DSC) is a thermoanalytical technique in which the difference in the amount of heat required to increase the temperature of a sample and reference is measured as a function of temperature. Both the sample and reference are maintained at nearly the same temperature throughout the experiment. Generally, the temperature program for a DSC analysis is designed such that the sample holder temperature increases linearly as a function of time. When a phase transition occurs in the

sample cell, there is a difference in the power needed to heat the two cells. The power required to maintain both cells at the same temperature is measured and converted to give an output of heat capacity versus temperature. The heat capacity versus temperature curve is analysed to determine the transition temperature, T_m , and the sharpness of the phase transition corresponds to the temperature width at half peak height $\Delta T_{1/2}$. DSC is as a sensitive and powerful tool for physicochemical characterization of liposomes. The shape of the heat capacity curve contains information about the phase transition itself, which includes both chemical and physical aspects.

Thermal analysis of MVL membranes was studied by DSC (DSC-50; Shimadzu, Japan). About 2.2–2.5 mg each sample was encapsulated in hermetically sealed standard aluminium DSC pans. The samples were heated from 10°C to 80°C at rate of 2°C min^{-1} . Empty aluminium pans were used as reference samples.

Preparation of topical hydrogel

Propyl and methyl paraben were dissolved in 20 ml distilled water in an aluminium foil-covered beaker. RB (0.01%) was added with gentle agitation. CMC (5%) was then added to the solution with continuous agitation at 50 rpm until swelling was complete. The mixture was left for 24 h at 4°C to ensure removal of air from the gel (gel containing free RB, F-RB). A similar gel formulation containing 0.01% RB in freshly prepared MVL (higher encapsulation capacity and smaller size) was prepared using the previous procedure (formulation MVL–RB IV).

Some pharmaceutical properties of the prepared hydrogels were evaluated including percent drug content, uniformity, pH, spreadability, drug release and some organoleptic characteristics such as tackiness, grittiness and transparency.

Hydrogel characterization

Determination of drug content, pH and spreadability

For determination of drug content, 1 g gel was weighed into a 100-ml volumetric flask and dissolved in HEPES buffer, and then diluted appropriately and analysed on a Shimadzu UV-1650 UV/VIS double beam spectrophotometer at a λ_{max} of 544 nm. To determine the spreadability of the gel, 0.5 g gel was placed within a circle of 1 cm diameter premarked on a glass plate over which a second glass plate was placed. A 500-g was rested on the upper glass plate for 5 min. The increase in diameter due to spreading of the gels was noted.

The pH of the 5% (w/w) gel was determined using a Corning pH meter standardized before use using pH 4.0 and 7.0 standard buffers.

In vitro release of RB from gel formulations

The F-RB gel containing free RB and the MVL-RB gel (1 ± 0.15 g of each) were placed in eight watchglasses each of 5 cm diameter and covered with a dialysis membrane of 0.5 mm pore size prewetted with HEPES buffer. The watchglasses were placed in 50 ml HEPES buffer of pH 5.5 (skin pH) at $32 \pm 0.5^\circ\text{C}$ (skin temperature) as acceptor solution. The acceptor solution was stirred with a paddle at a constant rate of 100 rpm in a dissolution test apparatus (TDT-08L; Electrolab, Mumbai, India) in which paddles were fitted to 100-ml glass dissolution vessels. Four samples of each type of gel were tested.

Release kinetics analysis

To study the mechanism of the RB release from MVL and from the prepared F-RB gel and MVL-RB gel, the release data were fitted to a zero-order, a first-order and Higuchi's diffusion control models using coefficient of variation for data analysis and Statistix for MS Excel software. The release kinetics were estimated by applying the highest linear correlation coefficient and the least coefficient of variation. The release rate constants from each formula were calculated.

RB penetration into mouse skin and photodynamic study

The distribution of RB in the skin after topical application in either the F-RB gel or the MVL-RB gel containing 0.01% RB was evaluated in healthy albino mice. The animals were treated following the standard regulations of the international institutional guidelines and guidelines set out in the Guide for the Care and Use of Laboratory Animals (NIH publication no. 96-03, 1996). A total of 45 male albino mice aged 25 ± 15 days and weighing 120 ± 20 g were used. They were divided into three groups, a control group, a group treated with free RB gel (F-RB group) and a group treated with the MVL-RB gel (MVL-RB group). The control group consisted of five mice. The F-RB group (20 mice) and the MVL-RB group (20 mice) were each subdivided into two further groups. After shaving the animals backs with an electric shaver, each subgroup was treated topically with 0.5 ± 0.05 mg of the appropriate gel formulation (F-RB or MVL-RB) which was left in place for 15 min or 30 min. Five animals in each subgroup were killed by overdose of general anaesthetic and a skin sample was taken using a 5-mm punch, fixed and mounted in paraffin without counterstaining for fluorescence microscopy. The other five mice in each subgroup were irradiated for 10 min with light of wavelength 550 nm emitted from an 80-mW LED (Photon Scientific, Egypt) at an energy density of 48 J/cm^2 . The

animals were killed and skin samples taken 24 h after irradiation. The samples were fixed and mounted in paraffin and stained with haematoxylin & eosin (H&E) for histological study.

Microscopy and fluorescence microscopy

A Carl Zeiss MicroImaging microscope (Carl Zeiss Micro-Imaging, Thornwood, NY) was used to examine and photograph the processed tissue sections (skin and underlying tissue of 5 μm thickness) using transmitted light bright field observation (halogen illumination), and an Olympus CKX41 inverted microscope with a mercury lamp fluorescence unit (U-RFLTSO) and a green filter cube (510–550 nm) for excitation and beyond 590 nm for emission was used to examine the depth of penetration of RB into the tissue by monitoring the emitted orange fluorescence of RB. The fluorescence images were acquired using a Canon PowerShot A650 IS digital camera.

This approach allowed RB present in the tissue to be readily imaged (as orange RB fluorescence on a dark background). Sections from the control animals which did not receive RB or H&E counterstaining showed no detectable autofluorescence.

Histological assessment of RB penetration

Fluorescence micrographs were examined to assess RB staining. The micrographs were scored as described previously [5]. Briefly, a scale of 0 (low) to 3 (high) was used to assign uniformity and density scores for the RB fluorescence of each specimen. Individual scores for uniformity and density were assigned for the stratum corneum, viable epidermis and dermis. Separate scores were then combined into a single metric (penetration index, PI) for each of these three layers; for example, for the stratum corneum: $PI_{SC} = (U_{SC} + D_{SC})/2$, where U_{SC} is the uniformity score and D_{SC} is the density score. Scores were recorded by two blinded readers and comparison with H&E-stained sections facilitated identification of major tissue structures.

Statistical analysis

One-way analysis of variance followed by the Tukey-Kramer multiple comparisons test using GraphPad Instat software v.2.05 was used to determine the statistical significance of the differences in encapsulation efficiency, release data and penetration index scores. All p values were two-tailed, and differences were considered significant when the p value was less than 0.05, and highly significant when less than 0.01. The final data are expressed as the means \pm standard deviation (SD).

Results

Characterization of MVL

Table 1 presents the characterization data of the prepared MVL formulations. Differences in lipid concentration did not affect the morphology of MVL. The prepared MVL were circular in shape and contained different numbers of concentric vesicles.

Particle size analysis showed a monomodal size distribution of the MVL formulations. The median particle size of the MVL formulations was in the range 2–4 μm . The minimum particle size was noted for the MVL-RB IV formulation which contained DPPC with lower CHOL and TP concentrations than the other formulations. In addition, the MVL-RB IV formulation showed significantly higher encapsulation efficiency (79%, $p < 0.05$) than the other formulations.

In vitro release kinetics

The in vitro release profiles of RB from MVL formulations are shown in Fig. 1. The amounts RB released within 2 h from the MVL-RB I, II and III formulations were not significantly different ($p > 0.05$; Table 1), but the amount released from the MVL-RB IV formulation was significantly higher than that from the other formulations ($p < 0.05$) as shown in Fig. 1. The release of RB from the MVL formulations was best fitted to Higuchi's diffusion model with a significantly higher diffusion rate constant ($p > 0.05$) ($K^{1/2} = 9.23 \pm 0.01$) than with the other formulations ($K^{1/2} = 3.94 \pm 0.021$, 3.2 ± 0.07 and 3.74 ± 0.03 for the MVL-RB I, II and III formulations, respectively), the rate constants of the latter formulations being not significantly different ($p > 0.05$).

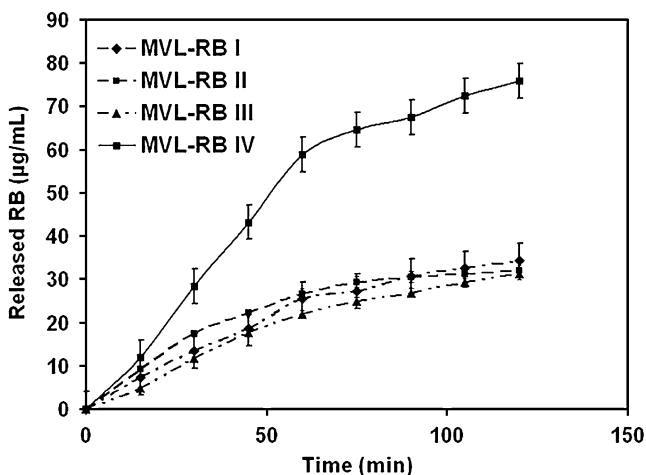


Fig. 1 Percentage RB released from MVL formulations in HEPES buffer (pH 7.4) at 37°C

Table 2 Phase transition temperatures and changes in peak half-widths of MVL formulations determined by DSC. The values are the means \pm SD from three parallel preparations

| MVL-RB formulation | T_m ($^{\circ}\text{C}$) | $\Delta T_{1/2}$ |
|--------------------|------------------------------|------------------|
| I | 59.83 ± 0.28 | 7.82 ± 0.3 |
| | 38.64 ± 0.1 | 7.5 ± 1.5 |
| II | 55.73 ± 0.31 | 23.1 ± 0.22 |
| III | 48.88 ± 0.3 | 7.3 ± 0.31 |
| | 58.5 ± 0.42 | 1.44 ± 0.18 |
| IV | 65.7 ± 0.6 | 1.9 ± 0.2 |
| | 28.57 ± 0.2 | 29.4 ± 4.6 |

Thermal analysis of MVL-RB

The phase transition parameters and the DSC thermograms of the MVL-RB formulations are shown in Table 2 and in Fig. 2, which show marked differences in transition positions. The CHOL to phospholipid ratio plays a significant role in the appearance, positions and peak intensities of T_m as indicated by $\Delta T_{1/2}$ values. As the forces between the bilayers increase, the cooperation between head groups and hydrocarbon tails of the phospholipid molecules involved in the melting process also increases, thus decreasing the temperature range and the half-width of the phase transition signals [26]. MVL-RB II with a lower ratio of solid lipids (CHOL and TP) to PC showed a shift of T_m to a higher temperature (55.73°C) and wide $\Delta T_{1/2}$ (23.1, MVL-RB II). While MVL formulations

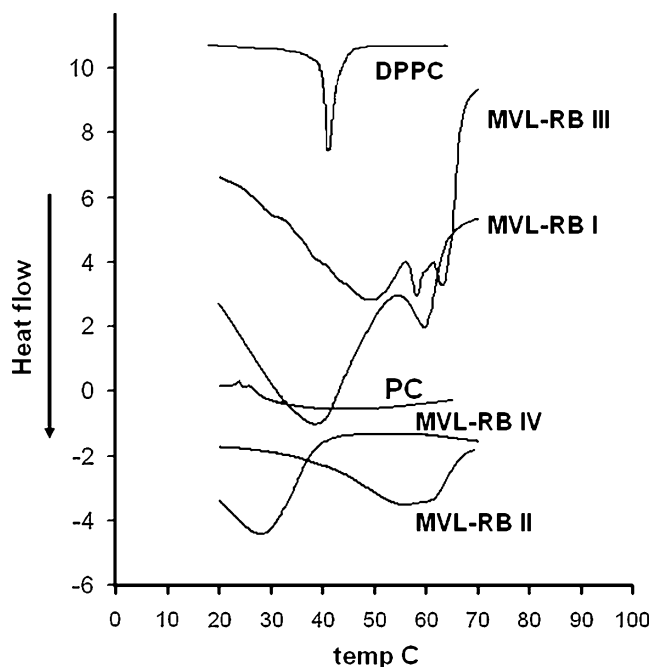


Fig. 2 DSC thermograms of the MVL-RB formulations

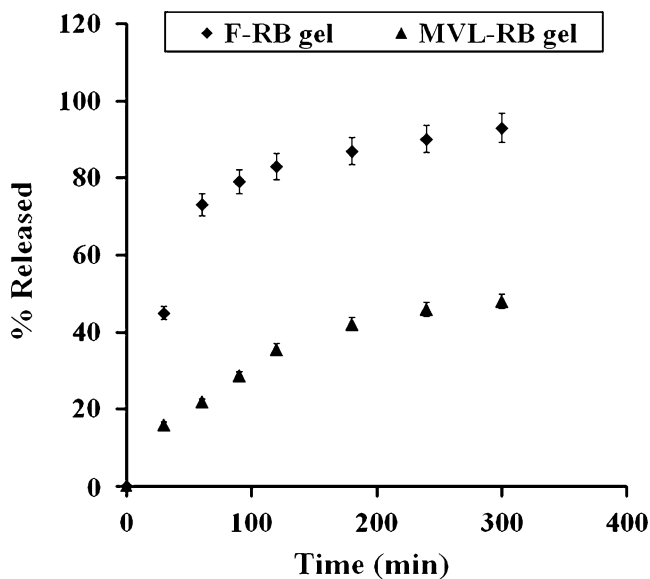


Fig. 3 RB release from F-RB and MVL-RB CMC hydrogels containing 0.01% RB in HEPES buffer (pH 5.5) at 36°C

containing DPPC (MVL-RB IV) showed a shift of T_m to a lower temperature (28.5°C) with a $\Delta T_{1/2}$ value of 29.4 reflecting lipid disruption [27]. On the other hand, MVL formulations with higher ratios of CHOL and TP to PC and DPPC (MVL-RB I and III) showed two T_m values (59.83°C and 38.64°C for MVL-RB I, PC MVL) and multiple T_m values (48.88°C, 58.5°C and 65.7°C for MVL-RB III, DPPC MVL).

Hydrogel characterization

The prepared F-RB gel and MVL-RB IV gel showed tackiness and a transparent appearance, and the drug was properly and uniformly dispersed. The drug contents of the F-RB and MVL-RB gels were $98.4 \pm 0.15\%$ and $99.6 \pm 0.1\%$, respectively. The pH value of the prepared gels was 7.6 ± 0.03 . Ideally a formulation should spread easily with maximum ‘slip’ and ‘drag’. In the spreadability tests, 0.5 g of each gel formulation in a circle of 1 cm diameter spread to a diameter of 5.8 cm, which is indicative of good spreadability of a CMC gel.

The release of RB from the two gel formulations is shown in Fig. 3. Significantly less RB was released from the MVL-RB formulation ($p > 0.01$) than from the F-RB formulation at all time points. Both formulations exhibited a linear release fitting Higuchi's diffusion mechanism with a slower release rate for the MVL-RB formulation ($K_{\text{MVL-RB}} = 2.8 \pm 0.05 \text{ min}^{1/2}$) than for the F-RB formulation ($K_{\text{F-RB}} = 3.3 \pm 0.08 \text{ min}^{1/2}$).

In vivo study

Fluorescence micrographs of histological sections of mouse skin taken 15 and 30 min after topical application of the F-

RB or MVL-RB gel are shown in Fig. 4. From the F-RB gel RB was delivered to the epidermis ($PI_{\text{ED } 30 \text{ min}} = 2.5 \pm 1.3$), but only weakly to the dermis ($PI_{\text{DE } 30 \text{ min}} = 1 \pm 1.2$). Significantly more RB was delivered to the dermis from the MVL-RB gel ($PI_{\text{DE } 30 \text{ min}} = 3 \pm 1.2$, $p < 0.05$) than from the F-RB gel.

As shown in Fig. 4 and Table 3, increasing the gel application time resulted in a marked increase in fluorescence intensity. Moreover, evident RB fluorescence was seen in the skin layers including the dermis following application of the MVL-RB gel, in contrast to the fluorescence seen following application of the F-RB gel which was restricted to the epidermis, reflecting the improvement in RB distribution through the skin layers when encapsulated in MVL. The stained histological sections of irradiated skin confirmed these observations. Sections of irradiated skin treated with F-RB showed necrotic hair follicles in the epidermis with a damaged stratum corneum indicating RB accumulation in the epidermal layers rather than in the dermal region as shown in Fig. 5b. On the other hand, sections of irradiated skin treated with MVL-RB displayed damaged and necrotic hair follicles located in the deep dermal layer while the stratum corneum remained intact, indicating the migration of MVL-RB into deeper skin layers (Fig. 5c).

Discussion

The MVL formulations loaded with RB were prepared by a w/o/w double emulsification method using natural PC,

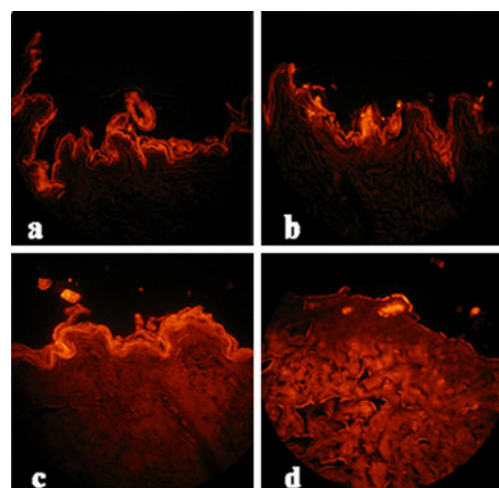


Fig. 4 Fluorescence micrographs of tissue sections showing RB penetration into the skin of normal albino mice ($\times 100$). **a, b** Skin treated with the F-RB gel containing 0.01% RB for 15 min (**a**) and 30 min (**b**) shows uniform staining of the epidermis which is clearly demarcated from the unstained dermis. **c, d** Skin treated with the MVL-RB gel containing 0.01% RB for 15 min (**c**) and 30 min (**d**) shows uniform distribution of RB in the dermis

Table 3 Penetration of RB into the skin after application of F-RB and MVL-RB gel containing 0.01% RB for 15 min and 30 min shown as values of PI determined from measured fluorescence intensities of RB

in 5-mm tissue sections. The values presented are the means \pm SD from three determinations recorded by two blinded readers

| Formulation | 15 min | | | 30 min | | |
|-------------|------------------|------------------|------------------|------------------|------------------|------------------|
| | PI _{SC} | PI _{ED} | PI _{DE} | PI _{SC} | PI _{ED} | PI _{DE} |
| F-RB | 2.5 \pm 1.58 | 2.5 \pm 1.2 | 0 | 2.5 \pm 1.7 | 2.5 \pm 1.3 | 1 \pm 1.2 |
| MVL-RB | 3 \pm 1.1 | 3 \pm 1.5 | 2 \pm 1.02 | 2 \pm 1.1 | 2.5 \pm 1.18 | 3 \pm 1.2 |

SC stratum corneum, ED epidermis, DE dermis

synthetic DPPC and CHOL. Lipid composition was altered with TP as an integral structural component leading to a unique MVL structure. The TP becomes part of the corner or edges where membranes meet and thus stabilizes the membrane boundaries [18].

DSC studies were performed in order to obtain a better understanding of the interactions of RB with the liposomal membrane and the effect of CHOL on MVL properties affecting the delivery of its content, and of the mechanism involved in skin absorption [27, 28]. PC and DPPC liposomes, due to their simplicity, have been used as a model membrane in many other studies [29–31]. Their transition temperatures (T_m) are characterized by narrow main endothermic peaks (gel-to-liquid crystalline phase), where the lipid acyl chains are undergoing a chain melting transition at the temperature T_m to a liquid crystalline phase [27, 31, 32]. The characteristic endothermic peak (Fig. 2) observed for the single system of DPPC is shifted to a higher temperature and broadened as the mole fraction of CHOL increased reflecting membrane rigidity. This effect on the main transition endotherm may be explained as a result of mixing of CHOL with DPPC, which may indicate closer packing of DPPC and CHOL molecules forming the

lamellar bilayers [33]. While at lower CHOL concentrations (MVL-RB IV) T_m is shifted to a lower temperature reflecting lipid disruption, in agreement with the significant increase in the amount of drug released compared with other formulations. The pronounced signals representing two transition temperatures showed for MVL-RB I and MVL-RB III is widely accepted. On the basis of both experimental [34, 35] and theoretical studies [36–38], the origin of this behaviour can be ascribed to phase separation, whereby phospholipid acyl chain melting transitions can arise both from CHOL-rich and CHOL-poor regions of the bilayer.

The slower RB release from the MVL-RB hydrogel than from the F-RB hydrogel can be attributed to the number of barriers to the diffusion pathways of the drug from MVL vesicles. The drug first passes through these compartments, then diffuses into the surrounding hydrogel network and to the external medium [24]. The observed trends for delivery of free RB to the epidermis are consistent with standard transdermal delivery models for hydrophilic agents [39]. Such agents must pass through the desiccated stratum corneum before they can reach significant concentrations in viable regions of the epidermis and beyond. The formula-

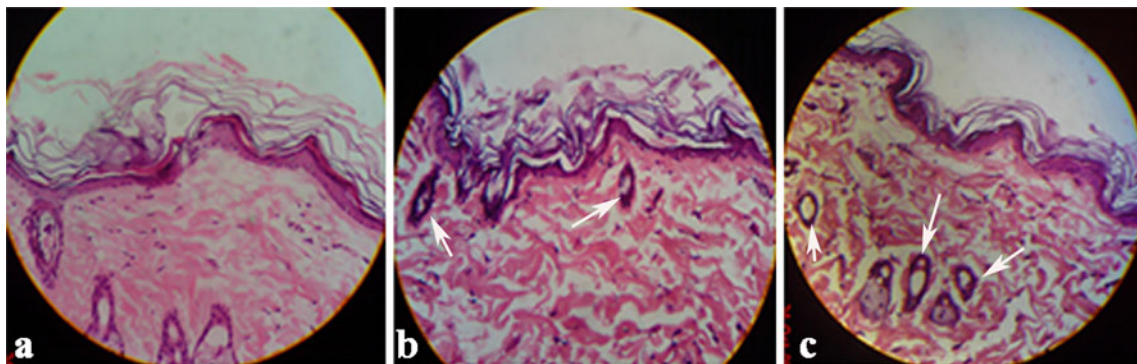


Fig. 5 H&E-stained sections under bright field observation (all $\times 100$). **a** Control section: a lightly stained stratum corneum is evident above a thicker, darkly stained viable epidermis. **b** Section of skin treated with F-RB hydrogel containing 0.01% RB for 30 min followed by irradiation with the 80-mW LED at 550 nm for 10 min (48 J): marked damage to the stratum corneum, superficial hair

follicles (arrows) and a normal dermis are apparent. **c** Section of skin treated with MVL-RB hydrogel containing 0.01% RB for 10 min followed by irradiation with the 80-mW LED at 550 nm for 10 min (48 J): normal stratum corneum and damaged hair follicles (arrows) in the deep dermis are apparent

tion of RB in hydrogels that do not interact with RB, such as CMC [40], may enhance RB delivery to the epidermis by improving contact between the skin surface and the applied surface reservoir of hydrated RB. Free RB did not penetrate beyond the epidermis as no detectable levels of RB were observed in the dermis by fluorescence microscopy and there was a sharp, clear demarcation of high levels of RB in the epidermis [5]. The hydrophobicity of MVL facilitates the migration of RB into deeper skin layers such that there was no RB accumulation in the epidermis and a clear demarcation of high levels of RB in the dermis.

Conclusion

From the present findings it can be concluded that MVL are promising depot delivery carriers for RB as a photosensitizer. Process parameters such as phospholipid type, amount of encapsulated RB and percentage of CHOL affect the packing properties of MVL and the interactions of the RB within the membrane, as well as the distribution of RB within the epidermal layers. CMC is an effective polymer for delivery of MVL in pharmaceutical topical hydrogels for medical use.

References

- Girotti AW (1990) Photodynamic lipid peroxidation in biological systems. *Photochem Photobiol* 51:497–509
- Davies MJ (2003) Singlet oxygen-mediated damage to proteins and its consequences. *Biochem Biophys Res Commun* 305:761–770
- Rossoni RD, Junqueira JC, Santos ELS, Costa ACB, Jorge AOC (2010) Comparison of the efficacy of Rose Bengal and erythrosin in photodynamic therapy against Enterobacteriaceae. *Lasers Med Sci* 25:581–586
- Bolean M, Paulino Tde P, Thedei G Jr, Ciancaglini P (2010) Photodynamic therapy with rose bengal induces GroEL expression in *Streptococcus mutans*. *Photomed Laser Surg* 1:S79–S84
- Wachter E, Dees C, Harkins J, Scott T, Petersen M, Rush R, Cada A (2003) Topical rose bengal: pre-clinical evaluation of pharmacokinetics and safety. *Lasers Surg Med* 32:101–110
- Lunardi CN, Tedesco AC (2005) Synergic photosensitizers: a new trend in photodynamic therapy. *Curr Org Chem* 9(8):813–821
- Tedesco AC, Rotta JCG, Lunardi CN (2003) Synthesis, photophysical and photochemical aspects of phthalocyanines for photodynamic therapy. *Curr Org Chem* 7:187–196
- Derycke AS, de Witte PA (2004) Liposomes for photodynamic therapy. *Adv Drug Deliv Rev* 56:17–30
- Vena FC, Turchiello RF, Laville I, Pigaglio S, Blais J, Tedesco AC (2004) 5-aminolevulinic acid ester-induced protoporphyrin IX in a murine melanoma cell line. *Lasers Med Sci* 19:119–126
- Sibata MN, Tedesco AC, Marchetti JM (2004) Photophysical and photochemical studies of zinc(II) phthalocyanine in long time circulation micelles for photodynamic therapy use. *Eur J Pharm Sci* 23:131–138
- Perugini PGI, Pavanetto F, Conti B, Scalia S, Baruffini A (2000) Study on glycolic acid delivery by liposomes and microspheres. *Int J Pharm* 196:51–56
- Lasic DD, Papadopoulos D (1995) Liposomes revisited. *Science* 267:1275–1276
- Meyer J, Whitcomb L, Collins D (1994) Efficient encapsulation of proteins within liposomes for slow release in vivo. *Biochim Biophys Res Commun* 199:433–438
- Kim T, Murdane S, Gruber A, Kim S (1996) Sustained-release morphine for epidural analgesia in rats. *Anesthesiology* 85:331–338
- Khatibi S, Howell SB, McCully C, Balis F, Poplack DG (1991) Prolongation of drug action in CSF by encapsulation into multivesicular liposomes. *Proc Am Soc Clin Oncol* 10:282–286
- Langston MV, Rampresad MP, Karali TT, Galluppi GR, Katre NV (2003) Modulation of the sustained delivery of myelopoietin (Leridistim) encapsulated in multivesicular liposomes (Depo-Foam). *J Control Release* 89:87–99
- Kim S, Turker MS, Chi EY, Sela S, Martin GM (1983) Preparation of multivesicular liposomes. *Biochim Biophys Acta* 728:339–348
- Spector MS, Zasadzinski JA (1996) Topology of multivesicular liposomes, a model biliquid foam. *Langmuir* 12(20):4704–4708
- Kim T, Kim J, Kim S (1993) Extended release formulation of morphine for subcutaneous administration. *Cancer Chemother Pharmacol* 33:187–190
- Kim S (1994) Depofoam mediated drug delivery into cerebrospinal fluid. *Methods Neurosci* 21:118–131
- Kim S, Howell S (1998) Multivesicular liposomes having a biologically active substance encapsulated therein in the presence of a hydrochloride. US Patent 5,807,572, 15 Sept
- Xiao CJ, Qi XR, Aini W, Wei SL (2003) Preparation of cisplatin multivesicular liposomes and release of cisplatin from the liposomes in vitro. *Yao Xue Xue Bao* 38:133–137
- Katre NV, Asherman J, Schaefer H, Hora M (1998) Multivesicular liposome (Depo Foam) technology for the sustained delivery of insulin like growth factor-I (IGF I). *J Pharm Sci* 87:1341–1345
- Jain SK, Jain RK, Chourasia MK, Jain AK, Chalasani KB, Soni V, Jain A (2005) Design and development of multivesicular liposomal depot delivery system for controlled systemic delivery of acyclovir sodium. *AAPS PharmSciTech* 6(1):E35–E41
- Cheng-Chung Chang, Yu-Tsai Yang, Jen-Chang Yangb, Hong-Da Wu, Tsuimin Tsaib (2008) Absorption and emission spectral shifts of rose Bengal associated with DMPC liposomes. *Dyes Pigment* 79:170–175
- Budai M, Szabó Zs, Szogyi M, Grof P (2003) Molecular interactions between DPPC and morphine derivatives: a DSC and EPR study. *Int J Pharm* 250:239–250
- El Maghraby GM, Campbell M, Finin BC (2005) Mechanisms of action of novel skin penetration enhancers: phospholipid versus skin lipid liposomes. *Int J Pharm* 305:90–104
- El Maghraby GM, Barry BW, Williams AC (2008) Liposomes and skin: from drug delivery to model membranes. *Eur J Pharm Sci* 34:203–222
- Auner BG, O'Neill MAA, Valenta C, Hadgraft J (2005) Interaction of phloretin and 6-ketocholestanol with DPPC-liposomes as phospholipid model membranes. *Int J Pharm* 294:149–155
- Lucio M, Bringezu F, Reis S, Lima JL, Brezesinski G (2008) Binding of nonsteroidal anti-inflammatory drugs to DPPC: structure and thermodynamic aspects. *Langmuir* 24:4132–4139
- Panicker L (2008) Interaction of propyl paraben with dipalmitoyl phosphatidylcholine bilayer: a differential scanning calorimetry and nuclear magnetic resonance study. *Colloids Surf B* 61:145–152

32. Wolka AM, Rytting JH, Reed BL, Finnin BC (2004) The interaction of the penetration enhancer DDAIP with a phospholipid model membrane. *Int J Pharm* 271:5–10
33. Krivanek R, Okoro L, Winter R (2008) Effect of cholesterol and ergosterol on the compressibility and volume fluctuations of phospholipid-sterol bilayers in the critical point region: a molecular acoustic and calorimetric study. *Biophys J* 94:3538–3548
34. McMullen TPW, Lewis RNAH, McElhaney RN (1993) Differential scanning calorimetric study of the effect of cholesterol on the thermotropic phase behaviour of a homologous series of linear saturated phosphatidylcholines. *Biochemistry* 32:516–523
35. Sankaram MB, Thompson TE (1991) Cholesterol-induced fluid-phase immiscibility in membranes. *Proc Natl Acad Sci U S A* 88:8686–8690
36. Ipsen JH, Karlström G, Mouritsen OG, Wennerstrom H, Zuckermann MJ (1987) Phase equilibria in the phosphatidylcholine-cholesterol system. *Biochim Biophys Acta* 905:162–172
37. Ipsen JH, Mouritsen OG, Bloom M (1990) Relationships between lipid membrane area, hydrophobic thickness, and acyl-chain orientational order. The effects of cholesterol. *Biophys J* 57:405–412
38. Ipsen JH, Mouritsen OG, Zuckermann MJ (1989) Theory of thermal anomalies in the specific heat of lipid bilayers containing cholesterol. *Biophys J* 56:661–667
39. Wester RC, Maibach HI (1995) Penetration enhancement by skin hydration. In: Smith EW, Maibach HI (eds) *Percutaneous penetration enhancers*. CRC Press, Boca Raton, pp 21–22
40. Tseng SC, Zhang SH (1995) Interaction between rose bengal and different protein components. *Cornea* 14:427–435